

undergo phosphine exchange with PMe_3 at rates that can be followed satisfactorily by $^{31}\text{P}\{^1\text{H}\}$ NMR spectroscopy.

Reaction with excess PMe_3 at low temperature in toluene forms the mixed-phosphine intermediates $\text{Mo}_2(\text{O}_2\text{CCMe}_3)_2\text{X}_2(\text{PMe}_2\text{Et})(\text{PMe}_3)$ before the second exchange occurs to give the fully substituted bis- PMe_3 product. The $^{31}\text{P}\{^1\text{H}\}$ spectra of the mixed-phosphine intermediates are characteristic of AB spin systems, with each phosphine resonance being split into a doublet of separation $^3J_{\text{pp}}$. The magnitude of the coupling constant reflects the trans-influence ability of the X group as shown in Table I. As X becomes a poorer trans-influence ligand, the molybdenum-phosphorus bond becomes stronger (as shown by the Mo-P bond lengths discussed above), and the phosphorus-phosphorus coupling constants increase. Thus, the trans-influence series alkyl > halide > amide > siloxide may be deduced for binuclear complexes of stereochemistry II.

Having established that the exchange process is stepwise, as was found in molecules of stereochemistry I,¹ we studied the kinetics of substitution for the first phosphine ligand as a function of the X group. We can minimize complications due to steric effects by choosing the two anionic groups at the extremes of Table I (CH_2CMe_3 and OSiMe_3), as they are very similar in size. Thus, the alkyl derivative $\text{Mo}_2(\text{O}_2\text{CCMe}_3)_2(\text{CH}_2\text{CMe}_3)_2(\text{PMe}_2\text{Et})_2$ reacts with an excess of PMe_3 at -30°C in toluene following first-order kinetics with $k_{\text{obsd}} = (1.00 \pm 0.05) \times 10^{-4} \text{ s}^{-1}$. No rate dependence on $[\text{PMe}_3]$ was observed over a range of 10–20 molar equiv/binuclear unit. An Arrhenius plot over three temperatures gave $\Delta H^\ddagger = 22.2 \text{ kcal mol}^{-1}$ and $\Delta S^\ddagger = 15 \text{ eu}$. The positive entropy of activation implies a dissociative mechanism for molecules of structure II, as observed previously for $\text{Mo}_2\text{Me}_4(\text{PR}_3)_4$.¹ The siloxide derivative $\text{Mo}_2(\text{O}_2\text{CCMe}_3)_2(\text{OSiMe}_3)_2(\text{PMe}_2\text{Et})_2$ reacts in a similar manner with PMe_3 , except that a higher temperature is necessary to achieve a similar rate. At 0°C , $k_{\text{obsd}} = (1.97 \pm 0.05) \times 10^{-4} \text{ s}^{-1}$, and Arrhenius parameters of $\Delta H^\ddagger = 24.7 \text{ kcal mol}^{-1}$ and $\Delta S^\ddagger = 15 \text{ eu}$ can be obtained.

Extrapolating the observed rate data to similar temperatures, we find that the phosphine dissociation rates are 10^2 times faster in the alkyl derivative than in the siloxide. This rate difference is most reasonably ascribed to a kinetic trans effect, where $\text{CH}_2\text{SiMe}_3 > \text{OSiMe}_3$ in a trans series. Hence the rate data, in conjunction with the structural and spectroscopic results, strongly indicate that both a trans influence and a trans effect are operating in these binuclear, quadruply bonded compounds.

Acknowledgment. We thank the NSF for departmental grants used to purchase the NMR spectrometers and X-ray diffractometer used in this work and Chevron (G.S.G.) and the UCB equal opportunity fund (V.V.M.) for fellowships. We also thank Dr. F. J. Hollander, staff crystallographer at the UCB X-ray crystallographic facility (CHEXRAY), for performing the X-ray study.

Registry No. $\text{Mo}_2(\text{O}_2\text{CCMe}_3)_2(\text{OSiMe}_3)_2(\text{PMe}_3)_2$, 80925-85-5; $\text{Mo}_2(\text{O}_2\text{CCMe}_3)_2(\text{CH}_2\text{CMe}_3)_2(\text{PMe}_3)_2$, 80925-86-6; $\text{Mo}_2(\text{O}_2\text{CCMe}_3)_2(\text{CH}_2\text{SiMe}_3)(\text{PMe}_2\text{Et})(\text{PMe}_3)$, 80925-87-7; $\text{Mo}_2(\text{O}_2\text{CCMe}_3)_2(\text{Me})_2(\text{PMe}_2\text{Et})(\text{PMe}_3)$, 80925-88-8; $\text{Mo}_2(\text{O}_2\text{CCMe}_3)_2\text{I}_2(\text{PMe}_2\text{Et})(\text{PMe}_3)$, 80925-89-9; $\text{Mo}_2(\text{O}_2\text{CCMe}_3)_2\text{Cl}_2(\text{PMe}_2\text{Et})(\text{PMe}_3)$, 80925-90-2; $\text{Mo}_2(\text{O}_2\text{CCMe}_3)_2\text{Br}_2(\text{PMe}_2\text{Et})(\text{PMe}_3)$, 80925-91-3; $\text{Mo}_2(\text{O}_2\text{CCMe}_3)_2(\text{N}(\text{SiMe}_2\text{H})_2)_2(\text{PMe}_2\text{Et})(\text{PMe}_3)$, 80925-92-4; $\text{Mo}_2(\text{O}_2\text{CCMe}_3)_2(\text{OSiMe}_3)_2(\text{PMe}_2\text{Et})(\text{PMe}_3)$, 80925-93-5; $\text{Mo}_2(\text{O}_2\text{CCMe}_3)_2(\text{CH}_2\text{CMe}_3)_2(\text{PMe}_2\text{Et})_2$, 80939-27-1; $\text{Mo}_2(\text{O}_2\text{CCMe}_3)_2(\text{OSiMe}_3)_2(\text{PMe}_2\text{Et})_2$, 80925-94-6; $\text{Mo}_2(\text{O}_2\text{CCMe}_3)_4$, 55946-68-4; PMe_3 , 594-09-2.

Supplementary Material Available: A listing of positional and thermal parameters and their estimated standard deviations (1 page). Ordering information is given on any current masthead page.

(10) The alkyl derivatives were prepared as in ref 2, the amide as in ref 3, and the halides as in ref 4. All compounds gave satisfactory elemental analysis, and NMR spectral properties (^1H , $^{13}\text{C}\{^1\text{H}\}$, and $^{31}\text{P}\{^1\text{H}\}$) show them to be of the structural type II.

Characterization of Several Novel Iron Nitrosyl Porphyrins

L. W. Olson,[†] D. Schaeper, D. Lançon, and K. M. Kadish*

Department of Chemistry, University of Houston
Houston, Texas 77004

Received November 16, 1981

Considerable attention has been given to the chemistry of synthetic transition-metal metalloporphyrins complexed by diatomic molecules.^{1,2} Because of their relevance to biological systems, the reactions of Fe(II) porphyrin complexes with diatomic molecules such as O_2 , CO, CS, and NO have been of special interest.

It has been reported³ that the five-coordinate complexes of PorFeNO (where Por = TPP²⁻ (tetraphenylporphyrin) or OEP²⁻ (octaethylporphyrin)) can be reversibly oxidized by cyclic voltammetry at a Pt electrode to yield $[\text{PorFeNO}]^+$. In this communication we report the isolation and characterization of a novel bis(nitrosyl) complex of Fe(III), $[\text{PorFe}(\text{NO})_2]^+$. We also report the reversible electrochemical reduction of PorFeNO to yield $[\text{PorFeNO}]^-$.

(TPP)FeNO and (OEP)FeNO are low-spin, five-coordinate complexes of Fe(II).²⁻⁴ Cyclic voltammetry of these complexes at a Pt electrode in CH_2Cl_2 , 0.1 M TBAP (tetra-*n*-butylammonium perchlorate), reveals that each neutral species undergoes a reversible one-electron oxidation and a reversible one-electron reduction during the time scale of the experiment. This is shown in Figure 1, and the potentials of the reactions are listed in Table I. Also listed in this table are potentials for several representative five- and six-coordinate complexes of (TPP)Fe and (OEP)Fe in both CH_2Cl_2 and pyridine. As seen from this table, the potentials for oxidation of PorFeNO are extremely positive and are, in fact, the most positive ever reported for the reaction $\text{Fe}(\text{II}) \rightleftharpoons \text{Fe}(\text{III})$. This substantial stability of the ferrous form is reflected in the relative inertness of PorFeNO to air oxidation and to displacement by other ligands.⁴ The differences between the OEP and TPP complexes reflect the greater basicity of the OEP²⁻ ring and are consistent with differences observed for other complexes of the two porphyrins.⁵

Oxidation of PorFeNO greatly increases the ability of the nitrosyl ligand. Attempts to isolate $[\text{PorFeNO}]^+$ by controlled-potential coulometry in CH_2Cl_2 at 1.0 V vs. SCE, 0.1 M TBAP, produced only PorFeClO_4 as determined by electronic spectra.⁶ However, electrolysis under an atmosphere of nitric oxide rather than nitrogen produced a new compound whose electronic spectrum is shown in Figure 2. Two Soret bands of significantly lowered intensity are observed for both OEP and TPP derivatives. Purging the solution with an inert gas results in appearance of the perchlorate spectrum. Conversely, exposure of solutions of PorFeClO_4 to nitric oxide regenerates the spectrum in Figure 2.

Crystalline solids may be obtained from CH_2Cl_2 /hexane solutions, but decomposition occurs unless they are stored under nitric oxide. Two N–O stretching frequencies in the infrared spectrum at 1940 and 1860 cm^{-1} (TPP derivative) provide evidence that this new species is the bis(nitrosyl) complex $[\text{PorFe}(\text{NO})_2]^+\text{ClO}_4^-$. The perchlorate region is typical of ionic rather than coordinated ClO_4^- .⁶ Conductivity studies in CH_2Cl_2 under NO show a molar conductivity of 40.8 $\Omega^{-1} \text{ cm}^2 \text{ mol}^{-1}$, consistent with a 1:1 electrolyte such as TBAP and much larger than a

[†] On leave of absence from Grand Canyon College, Phoenix, AZ 85017.

(1) "The Porphyrins"; D. Dolphin, Ed.; Academic Press: New York, 1979; Vol. 1–VII.

(2) Buchler, J. W.; Kokisch, W.; Smith, P. D. In "Structure and Bonding"; Bunitz, J. D., Ed.; Springer-Verlag: New York, 1978; Vol. 34.

(3) Buchler, J. W.; Kokisch, W.; Smith, P.; Tonn, B. Z. *Naturforsch.* B **1978**, *33b*, 1371.

(4) Wayland, B. B.; Olson, L. W. *J. Am. Chem. Soc.* **1974**, *96*, 6037.

(5) Fuhrhop, J. H. In "Porphyrins and Metalloporphyrins"; Smith, K. M., Ed.; Elsevier: New York, 1975; Chapter 14.

(6) Reed, C. A.; Mashiko, T.; Bentley, S. P.; Kastner, M. E.; Scheidt, W. R.; Spartalian, K.; Lang, G. *J. Am. Chem. Soc.* **1979**, *101*, 2948.

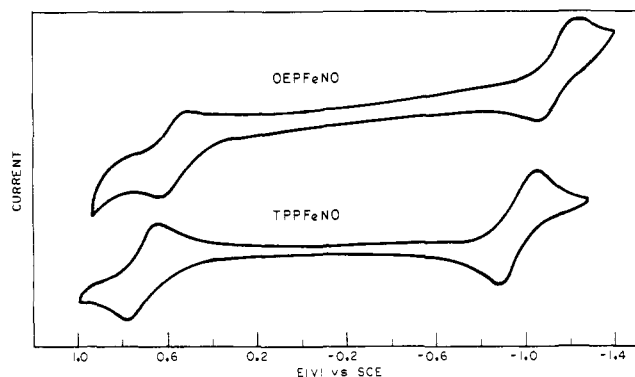


Figure 1. Cyclic voltammograms of (TPP)FeNO and (OEP)FeNO in CH_2Cl_2 , 0.1 M TBAP.

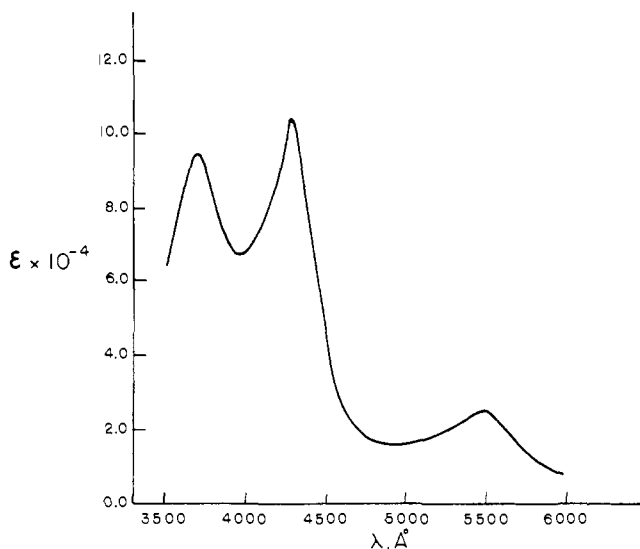


Figure 2. Electronic absorption spectra of 7.96×10^{-5} M $[(\text{TPP})\text{Fe}(\text{NO})_2]^+$ in CH_2Cl_2 , 0.1 M TBAP.

Table I. Reversible Half-Wave Potentials (V vs. SCE) for Reduction of Several Fe(III) and Fe(II) Complexes of TPP^{2-} and OEP^{2-} in CH_2Cl_2 and in Pyridine (0.1 M TBAP)

compd	CH_2Cl_2		pyridine	
	Fe(III)/Fe(II)	Fe(II)/Fe(I)	Fe(III)/Fe(II)	Fe(II)/Fe(I)
(TPP)FeNO	0.74 ^a	-0.93 ^b	0.54 ^g	-0.98 ^b
(OEP)FeNO	0.60 ^a	-1.10 ^b	0.57 ^g	-1.10 ^b
(TPP)FeClO ₄	0.22 ^c	-1.06 ^c	0.15 ^c	-1.50 ^c
(OEP)FeClO ₄	0.10 ^d	-1.29 ^d	-0.04 ^e	-1.68
(TPP)FeF	-0.50 ^c	-1.50 ^c	0.16 (-0.46) ^{c,f}	-1.50 ^c

^a Reference 2 and this work. ^b Reduction may actually involve orbitals of NO rather than the central metal. ^c Reference 8. ^d Reference 7. ^e Kadish, K. M.; Bottomley, L. A.; Kelly, S.; Schaeper, D.; Shiue, L. R. *Bioelectrochem. Bioenerg.* 1981, 8, 213. ^f Two different electrode processes occurred. ^g Irreversible reaction. The value presented is $E_{p,a}$.

nonelectrolyte such as (TPP)FeBr ($5.8 \Omega^{-1} \text{cm}^2 \text{mol}^{-1}$). A magnetic susceptibility of $2.0 \mu_B$, as determined by the Faraday method, indicates an $S = 1/2$ ground state. The electron spin resonance spectra of $[(\text{TPP})\text{Fe}(\text{NO})_2]^+$ shown in Figure 3 is similar to the ESR spectrum of (TPP)FeNO⁴ except that hyperfine splitting from both axial nitrogens is observed. The spectrum disappears when the nitric oxide atmosphere is removed, which is consistent with the electronic spectral changes indicating formation of $\text{PF}(\text{FeClO}_4)$.

Although cyclic voltammetry showed a well-defined, reversible one electron reduction of PorFeNO , electrolysis at -1.2 V vs. SCE in CH_2Cl_2 or pyridine did not provide isolation of $[\text{PorFeNO}]^-$.

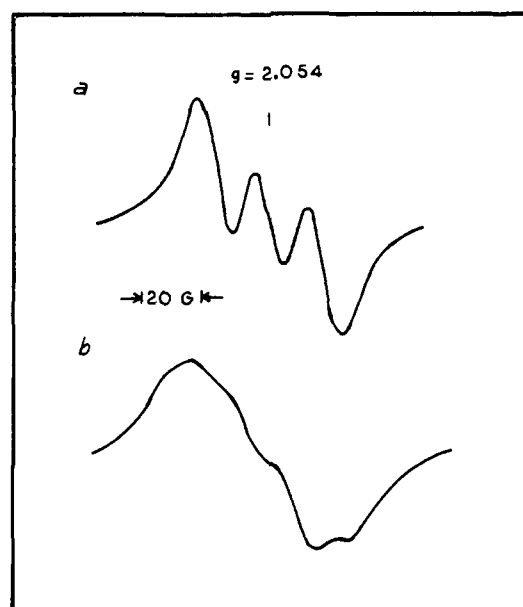


Figure 3. Isotropic ESR spectra of (a) (TPP)FeNO in toluene and (b) $[(\text{TPP})\text{Fe}(\text{NO})_2]^+$ in toluene under an atmosphere of nitric oxide.

Coulometric analysis for periods up to 3 h showed the addition of greater than 10 equiv of electrons, and electronic spectra showed only the starting material PorFeNO . Analysis of the current-time curves indicated the presence of a catalytic reaction in which $[\text{PorFeNO}]^-$ reacted with solvent, supporting electrolyte, or possible trace amounts of oxygen to regenerate the neutral Fe(II) nitrosyl complex. This catalytic regeneration of the starting material is not observed on the cyclic voltammetry time scale, as evidenced by the well-defined current-voltage curves shown in Figure 1.

It is interesting to note that the potential for reduction of (TPP)FeNO in CH_2Cl_2 is 130 mV more positive than that for reduction of (TPP)Fe in the absence of counterion and almost 600 mV more positive than that for reduction of (TPP)Fe(py)₂ or (TPP)FeF.⁷ Electronic absorption spectra of PorFeNO in CH_2Cl_2 /pyridine mixtures or neat pyridine are consistent with the formation of $\text{PorFeNO}(\text{py})$ in solution, which can be reduced to $[\text{PorFeNO}]^-$ or $[\text{PorFeNO}(\text{py})]^-$. The fact that even in neat pyridine the potential for reduction of PorFeNO [actually $\text{PorFeNO}(\text{py})$] is more positive than that for PorFe clearly demonstrates that the nitrosyl ligand is not lost during reduction. If this were the case, a potential in the neighborhood of -1.6 V would be predicted.

The odd electron in PorFeNO is known from ESR studies to occupy a bonding orbital with Fe d_{z^2} and σ_N character.⁴ Reduction of PorFeNO should place one electron in this σ -bonding orbital, which will be substantially delocalized onto the ligand. The relative ease of reduction of (TPP)FeNO (-0.93 V) in CH_2Cl_2 as compared to (TPP)Fe(II) (-1.06 V)⁷ or (TPP)Fe(py)₂ (-1.50 V)⁸ is consistent with the electron going into a bonding orbital. Oxidation of PorFeNO removes the single bonding electron with a consequent labilization of the nitrosyl ligand. Addition of a second nitric oxide molecule results in a low-spin complex, with occupation of the Fe d_{z^2} orbital as required by the appearance of hyperfine splitting in the ESR spectrum from the two axial nitrogens.

In summary, this study provides a new series of compounds that may be compared to their isoelectronic analogues among diatomic molecule complexes of metalloporphyrins. For example, $[\text{PorFeNO}]^+$ should be spin paired in analogy with PorFeCO^9 and have a linear Fe-N-O bond. The contrast in bonding and chemical

(7) Bottomley, L. A.; Kadish, K. M. *Inorg. Chem.* 1981, 20, 1348.

(8) Kadish, K. M.; Bottomley, L. A. *Inorg. Chem.* 1980, 19, 832.

(9) Wayland, B. B.; Mehne, L. F.; Swartz, J. J. *Am. Chem. Soc.* 1978, 100, 2379.

reactivity in a series such as $[\text{PorFe}(\text{NO})_2]^+$, $[\text{PorFeNO}]^+$, PorFeNO , and $[\text{PorFeNO}]^-$ provides a unique opportunity to evaluate the effect of changing only the number of electrons in the $[\text{PorFe}(\text{NO})_2]^+$ metal-ligand unit. Further crystallographic data will enhance this comparison.

Acknowledgment. We are grateful for the financial support of this work from the National Institutes of Health (Grant GM 25172). L.W.O acknowledges the support of the National Science Foundation (Grant SPI-8013117).

Registry No. $[(\text{TPP})\text{Fe}(\text{NO})_2]\text{ClO}_4$, 80964-55-2; $(\text{TPP})\text{FeNO}$, 52674-29-0; $(\text{OEP})\text{FeNO}$, 55917-58-3; $(\text{OEP})\text{FeClO}_4$, 50540-30-2.

Time-Resolved Resonance Raman Investigation of Photostimulated Electron Transfer from Amines to *trans*-Stilbene

Walter Hub, Siegfried Schneider, and Friedrich Dörr*

*Institut für Physikalische und Theoretische Chemie
der Technische Universität München
D-8046 Garching, West Germany*

J. Thomas Simpson, Joe D. Oxman, and Frederick D. Lewis*

*Department of Chemistry, Northwestern University
Evanston, Illinois 60201
Received August 31, 1981*

The formation of radical ion pairs via photostimulated electron transfer is a process of fundamental importance in photochemistry and photobiology. Fast transient electronic-absorption spectroscopy has been employed to study the formation and dynamics of radical ions;¹ however, the characterization of reactive intermediates from featureless absorption spectra is often less than fully satisfactory. Time-resolved resonance Raman (TR³) spectroscopy provides a powerful technique for both the characterization of reactive intermediates and the investigation of reaction dynamics.² We report preliminary results from our TR³ investigation of electron transfer from the tertiary amines ethyldiisopropylamine and 1,4-diazabicyclo[2.2.2]octane (Dabco) to the singlet state of *trans*-stilbene. These results provide the first experimental evidence for the formation of the stilbene radical anion via photostimulated electron transfer from an organic electron donor to singlet *trans*-stilbene and serve to elucidate the differences in chemical behavior between trialkylamines and Dabco with singlet stilbene.³

Both ethyldiisopropylamine and Dabco quench the fluorescence of singlet *trans*-stilbene with rate constants that exceed the rate of diffusion in acetonitrile solution ($2 \times 10^{10} \text{ M}^{-1} \text{ s}^{-1}$). The measured lifetime of *trans*-stilbene in acetonitrile solution ($\tau = 50 \text{ ps}^4$) and the Stern-Volmer quenching constants^{3c} for ethyldiisopropylamine (4.9 M^{-1}) and Dabco (8.0 M^{-1}) provide singlet quenching rate constants of 1×10^{11} and $2 \times 10^{11} \text{ M}^{-1} \text{ s}^{-1}$, respectively. These values may reflect static quenching which results from the high amine concentrations necessary for the observation of quenching of the short-lived stilbene singlet or, perhaps, weak ground-state complexation. Quenching of singlet stilbene by tertiary amines, including ethyldiisopropylamine, results in moderately efficient formation of stilbene-amine adducts and

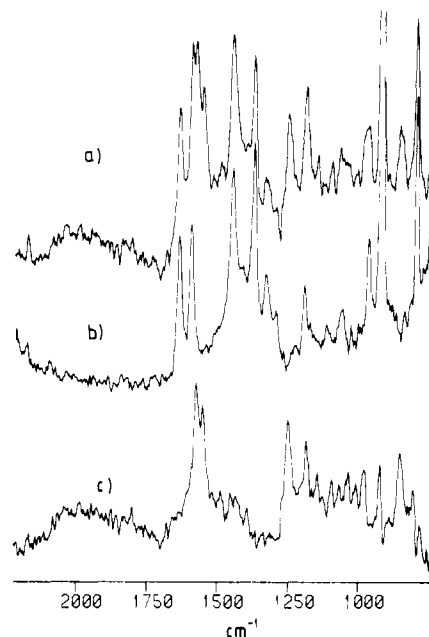
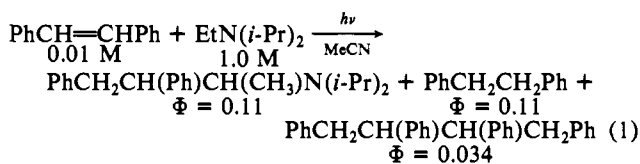


Figure 1. Raman spectrum of *trans*-stilbene (0.01 M) and Dabco (0.5 M) in acetonitrile solution: (a) 40 ns after photolysis pulse; (b) without preceding photolysis pulse; (c) difference spectrum due to the *trans*-stilbene anion radical.

reduced stilbene (eq 1); whereas, quenching by Dabco is not chemically productive.^{3c}



A deaerated acetonitrile solution of *trans*-stilbene (0.01 M) and Dabco (0.5 M) is irradiated at 337 nm with a pulsed nitrogen laser (1 mJ/pulse) at 298 K. After a time delay of Δt ns, the solution is irradiated at 484 nm with an excimer laser pumped dye laser (1 mJ/pulse). The Raman scattered light is spectrally resolved by a double-grating spectrograph (2 cm^{-1} resolution). After amplification in a gated image intensifier, the Raman spectra are recorded by means of an optical multichannel analyzer and stored in a computer for further data handling.⁵ Improvement in signal to noise ratio is achieved by sampling over approximately 500 excite-probe cycles. The Raman spectra obtained without and with photolysis ($\Delta t = 40 \text{ ns}$) are shown in Figure 1. Similar but more intense spectra are obtained for solutions of *trans*-stilbene (0.01 M) and ethyldiisopropylamine (1.0 M). Amine concentrations were selected to provide ca. 80% quenching of singlet *trans*-stilbene by both amines. The difference spectra shown in Figure 2 for singlet stilbene and ethyldiisopropylamine ($\Delta t = 100 \text{ ns}$, 500 ns, and 2.5 μs) demonstrate the absence of persistent Raman-active species. The frequencies and relative intensities of the prominent peaks in the difference spectra (Figures 1c and 2a; 1577, 1553, 1251, 1180, 979, 848, 625 cm^{-1}) correlate well with those previously reported by Takahashi and Maeda⁶ and by Dosser et al.⁷ for the anion radical of *trans*-stilbene.⁸

The time dependence of the stilbene anion radical signal intensity was determined by comparing the intensity of the

(1) Mataga, N.; Ottolenghi, M. "Molecular Association"; Foster, R., Ed.; Academic Press: London, 1979; Vol. 2, Chapter 1.

(2) For significant examples and leading references see: (a) Hub, W.; Schneider, S.; Dörr, F. *Angew. Chem., Int. Ed. Engl.* 1979, 18, 323-324. (b) Atkinson, G. H.; Dosser, L. R. *J. Chem. Phys.* 1980, 72, 2195-2197. (c) Beck, S. M.; Brus, L. E. *J. Am. Chem. Soc.* 1981, 103, 2495-2496. (d) Dallinger, R. F.; Farquharson, S.; Woodruff, W. H.; Rogers, M. A. *J. Ibid.* 1981, 103, 7433-7440.

(3) (a) Lewis, F. D. *Acc. Chem. Res.* 1979, 12, 152-158. (b) Lewis, F. D.; Ho, T.-I. *J. Am. Chem. Soc.* 1977, 99, 7991-7996. (c) Lewis, F. D.; Ho, T.-I.; Simpson, J. T. *J. Org. Chem.* 1981, 46, 1077-1082.

(4) Peters, K. S., private communication.

(5) For a description of the apparatus see: Dörr, F.; Hub, W.; Schneider, S. *J. Mol. Struct.* 1980, 60, 233-238.

(6) Takahashi, C.; Maeda, S. *Chem. Phys. Lett.* 1974, 28, 22-26.

(7) Dosser, L. R.; Pallix, J. B.; Atkinson, G. H.; Wang, H. C.; Levin, G.; Szwarc, M. *Chem. Phys. Lett.* 1979, 62, 555-561.

(8) The absence of peaks assignable to amine cation radicals is due to the lower (resonant) Raman scattering cross section of such species compared to the *trans*-stilbene anion radical. For the Raman spectrum of the Dabco cation radical see: Ernstbrunner, E. E.; Girling, R. B.; Grossman, W. E. L.; Hester, R. E. *J. Chem. Soc., Faraday Trans. 2* 1978, 74, 501-508.